21st Australasian Fluid Mechanics Conference
Adelaide, Australia
10-13 December 2018

# Observations of Near-bed Stress beneath Nonlinear Internal Wave Trains in the Ocean

**A.P Zulberti[1,2], G.N. Ivey[1,2] and N.L. Jones[1,2]**

[1]Oceans Graduate School
University of Western Australia, Crawley, Western Australia 6009, Australia

[2] Oceans Institute
University of Western Australia, Crawley, Western Australia 6009, Australia

## Abstract

Observations of near-bed turbulence are reported under the forcing of mode-1 nonlinear internal waves of depression in the Browse Basin on Australia's Northwest Shelf. These extreme events drive a fourfold increase in bed stress, and dominate sediment resuspension. Four methods for estimation of the bed stress were evaluated from near- seabed measurements in a total water depth of 250m. All four methods show a high level of agreement ($R^2$ above 0.91), suggesting that even in these highly complex flows, simple models based on the log-law of the wall or quadratic drag law may be useful for predicting sediment resuspension, provided measurements are made sufficiently close to the bed.

## Introduction

The interior of the density-stratified ocean is energised by atmospheric and astronomical forcing, giving rise to both barotropic and baroclinic flows whose energy ultimately decays through highly sheared turbulent motions. These flows apply loading on engineered structures as well as a direct shear stress on the ocean floor. This leads to mobilisation of sediment with important implications for the maintenance and operability of the pipelines and other engineering infrastructure on the continental shelf. Understanding the mechanisms controlling bed shear stress in shelf seas is a critical first step in evaluating sediment motion. This stress is typically evaluated using the log-law of the wall; the application of these concepts remains a topic of ongoing debate even for steady, unstratified, two dimensional flows (Marusic et al, 2013; George, 2007). The application of these ideas is further challenged in oceanic and environmental flows, where the influence of density stratification (eg. Perlin et al., 2007; Scully et al., 2011), strong acceleration (eg. Soulsby and Dyer 1981), vertical flows, and horizontal pressure gradients (Boegman and Ivey, 2009), introduce additional terms to the momentum equation which are not accounted for in simple log-law theory.

Evaluation of the applicability of the log-law in these complex flows has been inhibited by the lack of observations spanning the vast range forcing conditions found in shelf seas. In recent years, increased effort has been invested into characterising the structure of turbulence in well mixed tidal flows, owing to an increased appreciation for the significance of turbulence to tidal power generation (Milne, 2017; McCaffrey et al. 2015). By comparison, the structure of near-bed turbulence in deep, stratified, shelf flows - areas of particular interest to the offshore oil and gas industry - has received less attention.

We report here on observations from a 2017 field survey in which high resolution mean and turbulence measurements were made near the seabed under propagating nonlinear internal wave trains (NLIWs) on Australia's Northwest Shelf (NWS). These are three-dimensional, highly unsteady, stratified flows, which induce significant vertical velocities and horizontal pressure gradients; all of which influence the dynamics of the near-bottom flow in ways not yet characterised.

## Field Measurements

### Study site

The study site was located approximately 150 km east of Scott Reef in the Browse Basin on Australia's NWS (13.76°S 123.35°E). Measurements were made at a depth of 250 m on a gently sloping plateau (0.2 % gradient) which separates an inner and outer shelf break. The local barotropic tide at the site has a range of approximately 5 m, and generates a tidal ellipse with an approximately NW-SE oriented major axis, and a maximum spring velocity of approximately 0.4 $ms^{-1}$.

Regional three dimensional hydrostatic modelling has indicated two major regions for internal tide generation: one at the inner shelf break approximately 40 km to the south west, and one near the outer shelf break, approximately 100 km to the North West (Rayson et al., 2018).

### Instrumentation

A triangular array of conventional through water moorings was deployed to capture the external forcing, while a bottom mounted frame with a positively buoyant thermistor string was used to capture the mean and turbulent response of the boundary layer. The bottom mounted frame, deployed 50 m from the southernmost mooring, was equipped with two Nortek Vector ADVs, one 5 beam Nortek Signature 1000 broadband ADCP, an array of Seabird 56 thermistors, and a Seabird 39 temperature and pressure sensor. The two ADVs, mounted at 0.49 and 1.4 m above the seabed (ASB,) sampled at 64 Hz, while the ADCP sampled at 8 Hz, discretising the lower 20 m of the water column into 0.1 m bins starting at 0.55 m ASB. The Seabird 56 thermistors were approximately log-spaced with higher resolution near-bed, and sampled at 2 Hz. The Seabird 39 sampled at 15 seconds and was placed atop the thermistor string. The lander was equipped also with optical backscatter devices, including a Wetlabs FLNTUSB and a Sequoia LISST 200X mounted at 1.15 and 0.9 m ASB respectively.

The instruments recorded continuously from April 2 to May 1 2017, capturing the transition between the wet and dry seasons.

This transition resulted in a variable stratification over the period, and thus a variable baroclinic response to the action of the surface tide. More details of the through water column moorings, including instrument configuration, mooring locations, and analysis of NLIW characteristics, can be found in Rayson et al. (2018).

## Analysis

### Estimation of bed stress

Bed stress ($\tau_b$), in the form of a friction velocity, was estimated using four independent techniques. The first, which we denote as $u_*$, is by relation to the measured Reynolds stress from the ADV at 0.49 m:

$$\tau_b = \rho {u_*}^2 = \rho \left| \overline{u'w'} \right| \quad (1)$$

which assumes that the ADV at 0.49 m is located within a constant stress layer. The covariance in equation 1 was taken as total covariance between the vertical and streamwise fluctuations for the 64 Hz data. This was performed on 5 minute sections of data, overlapped by 80 % (i.e. centred every minute), and ultimately box-car filtered to provide a representative 5 minute value. Such an approach was necessary for the highly non-stationary NLIW forcing. The stream-wise direction was defined as the direction of the principal component of the full day's horizontal velocity record.

The second method, denoted $u_{*\varepsilon}$, uses the measured rate of turbulent kinetic energy (TKE) dissipation ($\varepsilon$):

$$u_{*\epsilon} = (\varepsilon \kappa z)^{1/3} \quad (2)$$

which assumes the vertical profile TKE dissipation scales with a single velocity profile and the distance to the bed. The dissipation of TKE was calculated using the inertial dissipation method (Bluteau et. al., 2011), using the same 5 minute segments as the Reynolds stress, and again boxcar filtered to a 5 minute average at 0.49 m ASB.

The third method, denoted $u_{*MF}$, uses the mean velocity and the log-law equation (Tennekes and Lumley, (1972)):

$$\frac{\overline{U}}{u_{*MF}} = \frac{1}{\kappa} ln\left(\frac{z u_{*MF}}{\nu}\right) + B \quad (3)$$

which assumes the results are measured within a true log-layer. We used the measured 5 minute mean velocity at 0.49 m ASB, von Karman's constant ($\kappa$) of 0.4, and a B of 5 wall units.

The fourth method, denoted $u_{*Cd}$, assumes that the mean velocity and friction velocity are scaled by a temporally constant drag coefficient (equation 4):

$${u_{*Cd}}^2 = C_d \overline{U}^2 \quad (4)$$

Though held constant in time, $C_d$ is dependent on the height above the bed. Following Soulsby (1983), we used a value of 0.0016 for sand/silt which applies at a height of 1 m ASB, and converted to a value of 0.00185 at the lower ADV height of 0.49 m using a log-law assumption.

## Results and Discussion

### Background forcing

The month-long deployment captured a wide variety of external forcing. The baroclinic tide had approximately equal energy to the barotropic forcing, which it lagged by approximately two days. Other features captured included mode-1 and mode-2 NLIWs, and the influence of a category 3 tropical cyclone (TC Frances). This paper focusses on a single day from the longer record (April 3 2017), in which a large mode 1 NLIW of depression passed during the barotropic flood (Figure 1a). The arrival times of this feature at the three moorings suggested the wave was propagating from the Northwest (Rayson et al., 2018). This is supported by the observed direction of the surface and near bed baroclinic currents.

The NLIW, which passed the mooring at approximately 0800 on April 3 induced vertical isotherm excursions of 100 m (Figure 1a), greatly intensified near-bed currents and modulated the thickness of the bottom mixed layer, which reached a minimum at the arrival of the leading crest (Figure 1b). The peak current magnitude during this event was approximately double the peak velocity on the opposite phase of the flow, in which no large NLIW was observed.

### Mean profiles near-bed

The mean velocity profiles within the lower ten metres had a highly complex structure compared to those of typical open channel or tidal channel flows. From 03:01 to 02:31, when the near bed currents were accelerating in the on-shelf direction, a bottom jet formed centred at 1 m ASB (Figure 2a). The lower, monotonically increasing portion of the profile grew in height, reaching a peak speed of 0.5 $ms^{-1}$ at approximately 5 m ASB. Beyond this peak, current magnitudes decreased approximately linearly before merging into the overlying flow. At the commencement of the deceleration period (03:21), evidence of the jet remained, yet the near-bed profiles appeared more linear (Figure 2a).

From 06:31 to 08:27, in the acceleration phase just prior to the arrival of the leading crest of the NLIW, another mild bottom jet formed growing to a peak magnitude of approximately 1 $ms^{-1}$ at approximately 4 m ASB (Figure 2b). Above the peak of the jet, velocities reduced over a few metres, then increased again into the overlying flow.

### Reynolds stress and friction velocity

Taking method 1 as a baseline, $u_*$ estimates ranged from $1\times10^{-3}$ to $3\times10^{-2}$ $ms^{-1}$, with the peak occurring during the first crest in the NLIW (Figure 3a). The remaining three methods showed a high level of agreement with this first method, with coefficients of determination above 0.91 (Figure 3b). The TKE dissipation method showed a high level of agreement across the full range of measured values with the mean value differing by less than 5% from the baseline. These results show that the key turbulent statistics of Reynolds stress and dissipation were well described by a single velocity scale ($u_*$) and the distance from the bed. Demonstrating this scaling supports the constant stress assumption, and hence the use of method 1 as the baseline method for bed stress estimation (equation 1).

With this baseline, bed stress estimates were between $1\times10^{-4}$ and $1\times10^{0}$ $kg.m^{-1}s^{-2}$ (Figure 4). The peak in bed stress under the passage of the first crest of the NLIW was a factor of four higher than the peak stress recorded during the on-shelf phase. The roughness Reynolds number calculated from these stresses and the characteristic sediment size from grab samples (not shown) supports the assumption of a hydrodynamically smooth bottom.

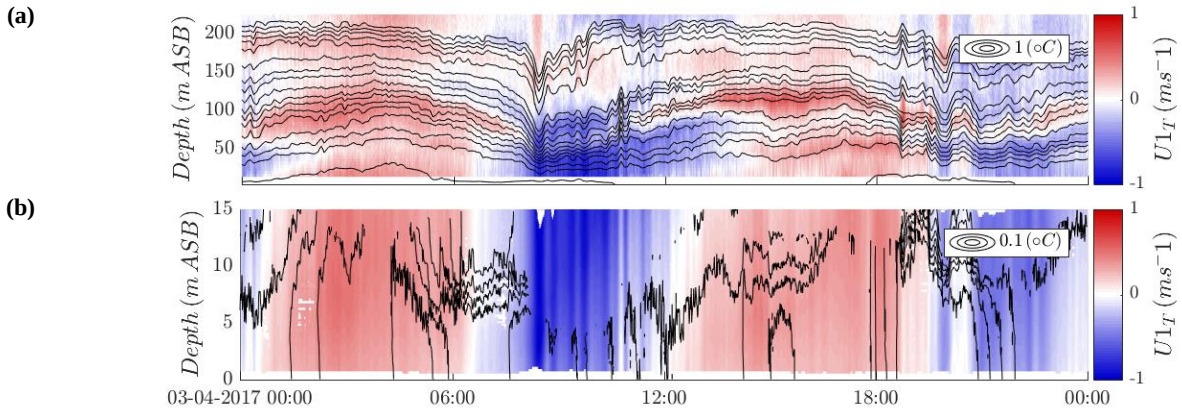


Figure 1 (a and b) Mean velocity profiles (coloured) and isotherms (black lines) on April 3. Velocities were rotated onto the direction of the principal horizontal current direction of the ADV at 0.49 m (denoted with the subscript 1). (a) shows the full water column measurements from the through water column mooring and (b) the near bed measurements from the bottom mounted lander frame.

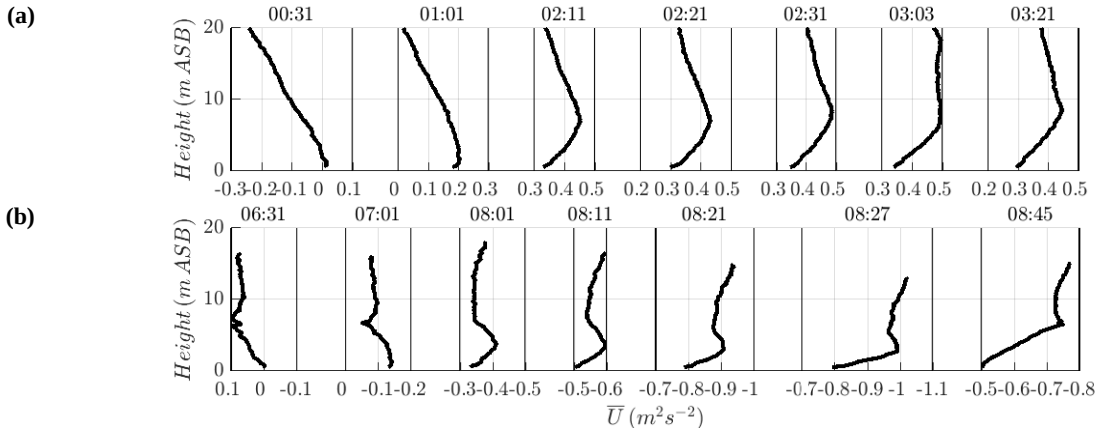


Figure 2 Mean profiles on April 3 during the: (a) acceleration phase of on-shelf flow near the bed and (b) acceleration phase prior to the arrival of a NLIW. Note that x-axes for (b) are reversed so that the flow develops from left to right in both instances.

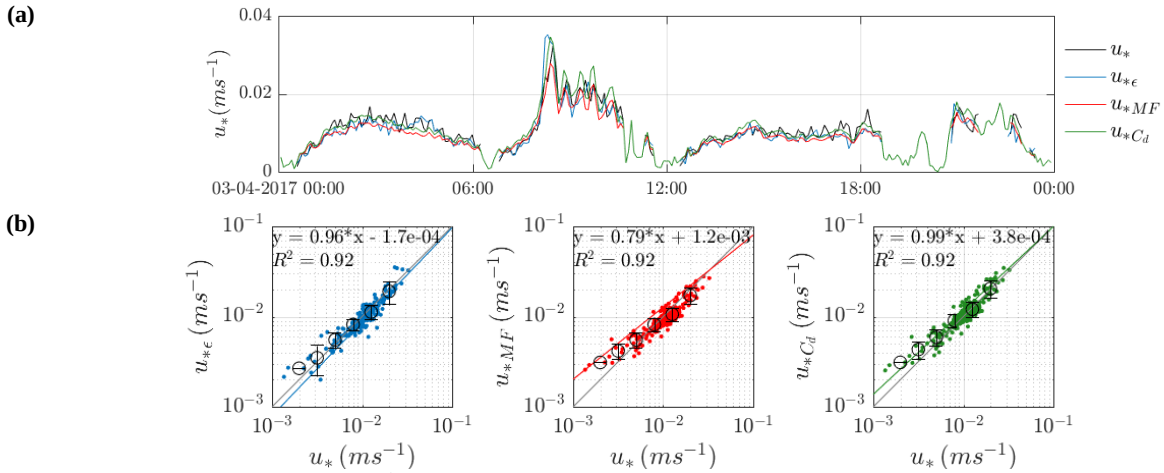


Figure 3 (a) Friction velocities ($u_*$) evaluated from the Reynolds stress (black), dissipation (blue), mean velocity (red) and the quadratic drag law (green) (b) Scatter plots of friction velocity ($u_*$) evaluated from the Reynolds stress against friction velocity ($u_*$) evaluated from (left) dissipation (centre) mean velocity, and (right) drag coefficient. Coloured dots represent individual samples, black circles represent means of binned data, and black bars represent the standard deviation of binned data.

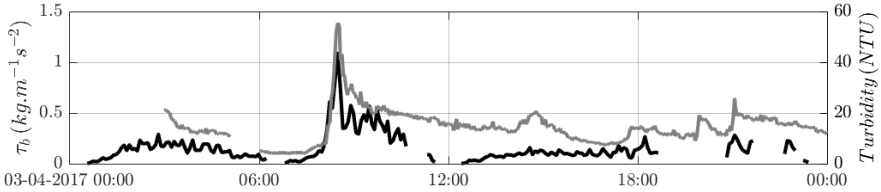


Figure 4 (b) Bottom stress ($\tau_b$, black) evaluated using equation 1 and turbidity at 1.15 m (grey). The first three hours of the turbidity record are excluded intentionally as the preceding friction velocity has influenced this part of the record.

The drag coefficient method also showed a high level of agreement across the full range of values, with a mean difference of only 4%. The drag coefficient method exhibited a large degree of scatter at low values around the time of flow reversal, however the turbulent velocities in these periods were typically non-stationary, and therefore these periods did not appear in the comparison. The high level of agreement therefore suggests that only that the quadratic drag law provides a reasonable estimate of bed stress where the turbulence is stationary.

The mean fit method under-predicted high values, and over-predicted low values. It also under-predicted the mean $u_*$ by around 11%. Similar to the drag coefficient method, the mean fit method exhibited larger scatter for at low friction velocities, though these could not be included in the comparison due to non-stationarity in the baseline.

It was somewhat surprising that the drag coefficient method, which has no Reynolds number dependence on the relation between mean flow and bed stress, out-performed the mean fit method. It must be noted however that both methods rely on empirical constants ($C_d$ or $B$) which have not yet been well established for this environment. We used the classical values of these constants in this study.

### Turbidity and suspended sediment

Turbidity measured at 1.15 m ASB, which can be assumed to scale linearly with suspended sediment concentration, was clearly related to the bed stress (Figure 4). The peak suspension event occurred during the passage of the leading crest of the NLIW, resulting in triple the sediment concentration at a height of 1.15 m compared with the opposite phase of the flow. Friction velocities for this event were above 0.01 $ms^{-1}$, and thus this event could be reliably predicted by all four methods.

The turbidity does not correlate perfectly with bed stress, as vertically integrated turbulent fluxes, mean advection, straining by the internal wave field and settling can also influence the recorded turbidity at 1.15 m ASB. These processes are the subject of future work.

## Conclusions

The four methods presented for estimating friction velocity show high agreement under propagating NLIWs, indicating that at this deep shelf sea site, distance to wall scaling provides a reasonable description of near-bed turbulence to a height of 0.49 m ASB, even under extreme conditions. Methods based on mean flow measurements proved as powerful as those based on turbulence measurements for the estimation of peak stresses, as required to predict the initiation of sediment motion. In the absence of turbulence measurements, however, it remains difficult to evaluate the assumption of constant stress, or the choice of empirical coefficients linking mean flow to bed stress. More work is required to provide guidance for the application of log-law to complex continental shelf flows.


## Acknowledgements

We thank the ARC Industrial Transformation Research Hub for Offshore Floating Facilities (IH140100012), and ARC Discovery Projects (DP140101322 and DP180101736). for funding this research. We thank also the staff at AIMS, crew of the R.V. Solander, and UWA staff and students for their assistance with the instrument deployment. A.Z. thanks Dr. Matt Rayson and Dr. Ian Milne for their discussions.


## References


[1] Bluteau, C. E., Jones, N. L., & Ivey, G. N., Estimating turbulent kinetic energy dissipation using the inertial subrange method in environmental flows, Limnology and Oceanography: Methods, **9**(7), 2011, 302-321.

[2] Boegman, L., & Ivey, G. N., Flow separation and resuspension beneath shoaling nonlinear internal waves, Journal of Geophysical Research: Oceans, 2009, **114**.

[4] George, W. K., Is there a universal log law for turbulent wall-bounded flows?, Philosophical Transactions of the Royal Society of London A: Mathematical, Physical and Engineering Sciences, **365**(1852), 2007, 789-806.

[5] Marusic, I., Monty, J. P., Hultmark, M., & Smits, A. J., On the logarithmic region in wall turbulence. Journal of Fluid Mechanics, **716**, 2013.

[7] McCaffrey, K., Fox-Kemper, B., Hamlington, P. E., & Thomson, J., Characterization of turbulence anisotropy, coherence, and intermittency at a prospective tidal energy site: Observational data analysis, Renewable Energy, **76**, 2015, 441-453.

[8] Milne, I. A., Sharma, R. N., & Flay, R. G. J., The structure of turbulence in a rapid tidal flow, Proc. R. Soc. A, **473**(2204), 2017, 20170295.

[9] Perlin, A., Moum, J. N., Klymak, J. M., Levine, M. D., Boyd, T., & Kosro, P. M,, A modified law-of-the-wall applied to oceanic bottom boundary layers, Journal of Geophysical Research: Oceans, **110**(C10), 2005.

[10] Rayson M.D., Jones, N.L., Ivey, G.I., Observations of large mode-2 nonlinear internal waves on the Australian North West Shelf. Manuscript submitted for publication, 2018.

[11] Scully, M. E., Geyer, W. R., & Trowbridge, J. H., The influence of stratification and nonlocal turbulent production on estuarine turbulence: An assessment of turbulence closure with field observations, Journal of Physical Oceanography, **41**(1), 2011. 166-185.

[12] Soulsby, R. L., & Dyer, K. R., The form of the near-bed velocity profile in a tidally accelerating flow. Journal of Geophysical Research: Oceans, **86**(C9), 1981, 8067-8074.

[13] Soulsby, R.L. The Bottom Boundary Layer of Shelf Seas, in Physical Oceanography of Coastal and Shelf Seas, editor B. Johns, Elsevier, 1983, 189-266

[14] Tennekes, H., Lumley, J. L., & Lumley, J. L., A first course in turbulence. MIT press, 197